Kinetics and Product Study of the OH- and NO_2-Initiated Oxidation of 2,4-Hexadiene in the Gas Phase

Michael E. Jenkin,*,† Malene Sørensen,‡ Michael D. Hurley,§ and Timothy J. Wallington§

Department of Environmental Science and Technology, Imperial College London, Silwood Park, Ascot, Berkshire, SL5 7PY, United Kingdom, Department of Chemistry, University of South Denmark, Campusvej 55, DK-5230 Odense M, Denmark, and Ford Research Laboratory, Ford Motor Company, SRL-3083, Post Office Box 2053, Dearborn, Michigan 48121-2053

Received: January 9, 2003; In Final Form: April 24, 2003

The kinetics and products of the OH- and NO_2-initiated oxidation of 2,4-hexadiene have been investigated at 296 K and 700 Torr by long-path Fourier transform infrared (FTIR) spectroscopy. Relative rate methods were employed for the photolysis of 2,4-hexadiene/CH_3ONO/NO/air mixtures to measure k(OH + 2,4-hexadiene) = $(1.76 \pm 0.58) \times 10^{-10}$ cm^3 molecule^{-1} s^{-1}. The OH-initiated oxidation of 2,4-hexadiene gave acetaldehyde, *trans*-crotonaldehyde, and 2,5-dimethylfuran, with molar yields of (30.6 ± 5.0)%, (12.9 ± 2.0)%, and (5.6 ± 1.0)%, respectively. These products suggest that the OH-initiated oxidation of 2,4-hexadiene proceeds, at least partially, by pathways analogous to those reported for 1,3-butadiene and isoprene. From the pseudo-first-order decay of 2,4-hexadiene in the presence of excess NO_2, a value of k(NO_2 + 2,4-hexadiene) = $(3.11 \pm 0.18) \times 10^{-19}$ cm^3 molecule^{-1} s^{-1} was derived. The reaction stoichiometry and products were investigated in the absence of O_2, in the presence of O_2, and in the presence of O_2 and NO. Reaction mechanisms consistent with the observations are presented. In the presence of NO and O_2, the NO_2-initiated chemistry leads to NO-to-NO_2 conversion, and the formation of HO_x radicals in significant yield, such that 2,4-hexadiene removal occurs by reaction with both NO_2 and OH. The results are consistent with HO_x yields of up to 0.75 ± 0.05, depending on the experimental conditions. The results also suggest that the nitrate forming channels account for (25 ± 5)% of the reactions of NO with peroxy radicals formed from the reactions of both OH and NO_2 with 2,4-hexadiene. The implications of the results are discussed within the context of the atmospheric chemistry of conjugated dienes. As part of this work, rate coefficients were determined for the reactions of NO_2 with 1,3-butadiene and styrene and for NO with 2,4-hexadiene: k(NO_2 + 1,3-butadiene) = $(2.54 \pm 0.15) \times 10^{-20}$, k(NO_2 + styrene) = $(1.4 \pm 0.3) \times 10^{-20}$, and k(NO + 2,4-hexadiene) ≤ 2×10^{-21} cm^3 molecule^{-1} s^{-1}.

1. Introduction

Conjugated dienes play a major role in the chemistry of the atmosphere. Isoprene (2-methyl-1,3-butadiene) is emitted in substantial quantities from biogenic sources and has the highest global mass emissions of all nonmethane hydrocarbons.[1] Conjugated dienes are also emitted as components of vehicle exhaust or fuel vapor,[2−4] and the detection of several conjugated dienes (including 2,4-hexadiene) in the urban environment has been reported.[5] A detailed knowledge of the atmospheric chemistry of conjugated dienes is therefore a necessary prerequisite to understanding tropospheric chemistry on a number of geographical scales.

It is well established that conjugated dienes react rapidly with OH radicals, NO_3 radicals, and ozone,[6] although reaction with OH tends to be the major atmospheric sink. The reactions with NO_2 have also received attention due to their importance under conditions typically employed in laboratory chamber systems,[7,8] and their possible role in thermal initiation of free radical catalyzed NO-to-NO_2 conversion during urban winter pollution episodes.[3,9] Whereas kinetics data are available for reactions of OH and NO_2 with a number of conjugated dienes,[6,10] product studies for the OH-initiated oxidation appear to be limited to 1,3-butadiene[11,12] and isoprene.[8,13−17] There is limited information available on the products and mechanisms of the NO_2-initiated oxidation of conjugated cyclic dienes. Atkinson et al.[7] reported evidence for the formation of a number of oxidized organic nitrogen compounds from the reaction of NO_2 with 1,3-cyclohexadiene and demonstrated that OH radicals were formed when NO was added to the system. Subsequently, Shi and Harrison[3] reported that the NO_2-initiated oxidation of 1,3-cyclohexadiene and 1-methyl-1,3-cyclopentadiene under simulated urban episode conditions leads to oxidation of NO to NO_2.

In the present paper, we report the results of an investigation of the kinetics and products of the reactions of OH and NO_2 with 2,4-hexadiene, using long-path Fourier transform infrared (FTIR) spectroscopy. The objectives of this work were to extend the available database on the atmospheric chemistry of conjugated dienes in general, and to gain further information on the their ability to generate HO_x radicals upon reaction with NO_2.

2. Experimental Section

All experiments were performed in the Ford 140-L Pyrex chamber, interfaced with a Mattson Sirius 100 FTIR spectrometer, which is described in detail elsewhere.[18] The chamber is

* To whom correspondence should be addressed: m.jenkin@imperial.ac.uk.
† Imperial College London.
‡ University of South Denmark.
§ Ford Motor Company.

10.1021/jp034053p CCC: $25.00
Published on Web 07/08/2003

equipped with 22 fluorescent blacklamps (GE F40BLB), emitting near-UV radiation in the range 300−450 nm. For the OH-initiated studies, OH radicals were thus generated by the photolysis of CH_3ONO in the presence of NO and O_2 by the well-established mechanism:

$$CH_3ONO + h\nu \rightarrow CH_3O + NO \quad (1)$$

$$CH_3O + O_2 \rightarrow HCHO + HO_2 \quad (2)$$

$$HO_2 + NO \rightarrow OH + NO_2 \quad (3)$$

The NO_2-initiated studies were carried out in the dark. Infrared spectra of reagents and products were derived from 32 coadded interferograms with a spectral resolution of 0.25 cm^{-1}, and an analytical path length of 27.1 m. All experiments were carried out at 296(±2) K and 700 Torr total pressure.

The organic reagents 2,4-hexadiene (≥99%, isomeric distribution unknown), styrene (≥99%), cyclohexene (≥99%), 1,3-butadiene (≥99%), acetaldehyde (≥99.5%), *trans*-crotonaldehyde (≥99.5%), and 2,5-dimethylfuran (≥99%) were obtained from Aldrich Chemical Co. NO, NO_2, O_2, N_2, and air were obtained from Michigan Airgas at research-grade purity. CH_3ONO was synthesized by the dropwise addition of 50% H_2SO_4 to methanol saturated with sodium nitrite. It was dried by passing through a column of $CaCl_2$, purified by fractional distillation, and stored in the dark at 296 K prior to use. Reference spectra were obtained by expanding calibrated volumes into the chamber. Allowance was made for dimerization of NO_2 in the calibrated volumes prior to addition to the chamber, by use of the expression given in the Appendix. Unless otherwise specified, all quoted errors are two standard deviations.

3. Results and Discussion

3.1. Kinetics of the Reaction of OH with 2,4-Hexadiene. The kinetics of reaction 4 were measured relative to those of reactions 5−7:

$$OH + \text{2,4-hexadiene} \rightarrow \text{products} \quad (4)$$

$$OH + \text{styrene} \rightarrow \text{products} \quad (5)$$

$$OH + \text{cyclohexene} \rightarrow \text{products} \quad (6)$$

$$OH + \text{1,3-butadiene} \rightarrow \text{products} \quad (7)$$

Initial reagent concentrations were 25−50 mTorr of 2,4-hexadiene, 10−50 mTorr of CH_3ONO, 25−60 mTorr of NO, and 7−15 mTorr of either styrene, cyclohexene, or 1,3-butadiene in 700 Torr of air diluent.

The observed loss of 2,4-hexadiene due to reaction with OH, versus those of the reference compounds used in the present work following UV irradiation of 2,4-hexadiene/reference/CH_3ONO/NO/air mixtures, is shown in Figure 1. The data have been corrected to account for the loss of 2,4-hexadiene via reaction with NO_2 accumulating in the system:

$$NO_2 + \text{2,4-hexadiene} \rightarrow \text{products} \quad (8)$$

Corrections were in the range 1−25% and were computed from $k_8 = 3.11 \times 10^{-19}$ cm^3 $molecule^{-1}$ s^{-1}, as determined in the present study (see section 3.3), the elapsed time during the experiment, and the average NO_2 concentration in the chamber during the experiment (measured by FTIR spectroscopy). Minor corrections (0.5−1.5%) for loss of styrene and 1,3-butadiene via reaction with NO_2

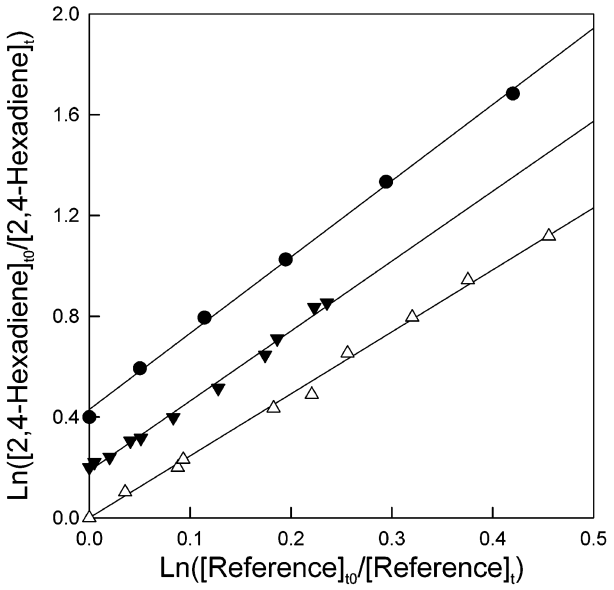

Figure 1. Loss of 2,4-hexadiene versus reference compounds (styrene, ●; cyclohexene, ▼; 1,3-butadiene, △) following exposure to OH radicals in 700 Torr of air. For clarity the data for styrene and cyclohexene references have been shifted vertically by 0.4 and 0.2 unit, respectively.

$$NO_2 + \text{styrene} \rightarrow \text{products} \quad (9)$$

$$NO_2 + \text{1,3-butadiene} \rightarrow \text{products} \quad (10)$$

were also applied by use of $k_9 = 1.4 \times 10^{-20}$ cm^3 $molecule^{-1}$ s^{-1} (derived from one experiment with a styrene/NO_2/air mixture in the present work; estimated uncertainty is ±20%) and $k_{10} = 2.54 \times 10^{-20}$ cm^3 $molecule^{-1}$ s^{-1}, as determined in the present study (see section 3.3). The plots in Figure 1 are linear and pass through the origin (allowing for vertical shift of the data for clarity of presentation) within the experimental uncertainties.

Least-squares analysis of the data in Figure 1 gives $k_4/k_5 = 3.03 \pm 0.12$, $k_4/k_6 = 2.75 \pm 0.20$, and $k_4/k_7 = 2.47 \pm 0.10$. Quoted uncertainties are two standard deviations from the linear regressions. Using $k_5 = (5.80 \pm 1.16) \times 10^{-11}$, $k_6 = (6.77 \pm 1.69) \times 10^{-11}$, and $k_7 = (6.66 \pm 1.33) \times 10^{-11}$ cm^3 $molecule^{-1}$ s^{-1} (recommended by Calvert et al.[6,19]) gives independent determinations of $k_4 = (1.76 \pm 0.36) \times 10^{-10}$, $(1.86 \pm 0.48) \times 10^{-10}$, and $(1.65 \pm 0.34) \times 10^{-10}$ cm^3 $molecule^{-1}$ s^{-1}. We choose to quote a value for k_4 which is the average of those determined with the three different reference compounds together with error limits that encompass the extremes of the individual determinations. Hence, $k_4 = (1.76 \pm 0.58) \times 10^{-10}$ cm^3 $molecule^{-1}$ s^{-1}. This result is consistent, within the experimental uncertainties, with the reported measurement of $k_4 = (1.34 \pm 0.27) \times 10^{-10}$ cm^3 $molecule^{-1}$ s^{-1} by Ohta,[20] based upon $k_7 = 6.66 \times 10^{-11}$ cm^3 $molecule^{-1}$ s^{-1}.

3.2. Products and Mechanism of the Reaction of OH with 2,4-Hexadiene. The products generated during the photolysis of 2,4-hexadiene/CH_3ONO/NO/air mixtures were investigated in a series of experiments. Initial reagent concentrations were 50−100 mTorr of 2,4-hexadiene, 10−60 mTorr of CH_3ONO, and 15−30 mTorr of NO in 700 Torr of air diluent. Acetaldehyde, *trans*-crotonaldehyde, and 2,5-dimethylfuran were detected as oxidation products. Following correction for 2,4-hexadiene removal via reaction with NO_2 (as described in the previous subsection), molar yields of (30.6 ± 5.0)%, (12.9 ± 2.0)%, and (5.6 ± 1.0)% were determined for acetaldehyde, *trans*-croton-

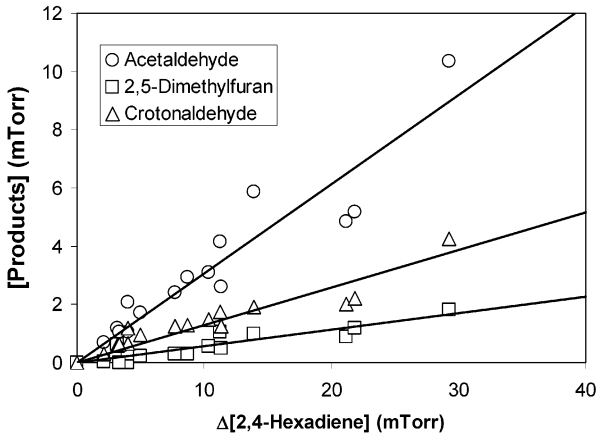

Figure 2. Formation of acetaldehyde, *trans*-crotonaldehyde, and 2,5-dimethylfuran relative to loss of 2,4-hexadiene at 296 K in 700 Torr of O_2, during photolysis of CH_3ONO/2,4-hexadiene/NO/O_2 mixtures. Data have been corrected for loss of 2,4-hexadiene by reaction with NO_2.

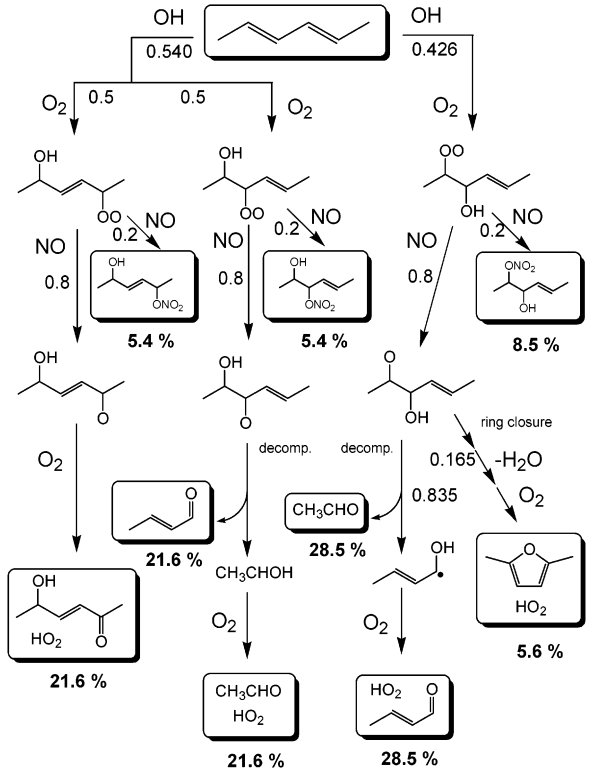

Figure 3. Schematic representation of possible pathways following the addition of OH to 2,4-hexadiene in the presence of NO and O_2 (for clarity, only trans isomers are shown). Assigned branching ratios are estimates, based on various sources of information as described in the text. Percentages are thus predicted molar yields of boxed products relative to 2,4-hexadiene lost. As discussed in the text, the predicted yields shown do not fully match those found experimentally.

aldehyde, and 2,5-dimethylfuran, respectively (see Figure 2), which are believed to result from the OH-initiated chemistry in the presence of NO. As discussed further in section 3.4, these products are not believed to be generated in significant yield from the NO_2-initiated chemistry alone.

A probable oxidation mechanism following the reaction of OH with 2,4-hexadiene in the presence of NO is illustrated in Figure 3. This is largely defined by analogy with those reported previously for isoprene[17,21,22] and 1,3-butadiene[11,22] and accounts qualitatively for the observed products. The branching ratios displayed in the figure for the various reaction channels have been estimated on the basis of a number of sources of information. The structure−reactivity relationships reported by Peeters and co-workers[23,24] for the reactions of OH with conjugated dienes suggest a minor contribution (3.4%) from abstraction of hydrogen from the terminal CH_3- groups, with 2- and 3-hydroxy addition collectively dominating and being of comparable importance. In the case of 2-hydroxy addition, the resultant radical possesses an allyl resonance, such that there are two possible positions for subsequent addition of O_2. Given that each of the peroxy radicals potentially formed is secondary, it seems reasonable to assume that the probability of O_2 addition is equivalent at both positions.

The various peroxy radicals (RO_2) generated following the initial attack of OH are expected to react with NO via two possible channels:

$$RO_2 + NO \rightarrow RO + NO_2 \quad (11a)$$

$$\rightarrow RONO_2 \quad (11b)$$

On the basis of reported information for 1,3-butadiene[11] and isoprene,[8] and for C_6 secondary alkyl peroxy radicals,[25] it seems likely that the nitrate-forming route (eq 11b) will make a minor but significant contribution, probably accounting for ca. 20% of the reaction in each case.

The subsequent fate of the RO radicals, formed from reaction 11a, is a major factor in determining the distribution of oxidized products. The 2-hydroxy-4-hexenyl-3-oxy and 3-hydroxy-4-hexenyl-2-oxy radicals are expected to undergo rapid decomposition, leading to the formation of acetaldehyde and the crotonaldehyde isomers, as shown in Figure 3. Such reactions are usually the dominant fate for β-hydroxyalkoxy radicals.[26] The formation of 2,5-dimethylfuran following the minor cyclization reaction of the 3-hydroxy-4-hexenyl-2-oxy radical is based on the route postulated by Atkinson et al.[13] to explain the formation of furan and 3-methylfuran in the 1,3-butadiene and isoprene systems. The 2-hydroxy-3-hexenyl-5-oxy radical is expected to yield an undetected hydroxyketone product, 5-hydroxy-3-hexen-2-one, either from direct reaction with O_2 or possibly (in the case of the cis isomer) from a 1,5 H atom shift isomerization, followed by reaction with O_2. This is analogous to the observed formation of hydroxycarbonyls in the OH-initiated oxidation of 1,3-butadiene[11] and isoprene.[16]

The reaction branching ratios given in Figure 3 lead to predicted molar yields of both acetaldehyde and crotonaldehyde of ca. 50%. Not only are these values significantly greater than those observed, but they also emphasize that the mechanism, as shown, must generate identical yields of acetaldehyde and crotonaldehyde. The nonequivalence of the observed yields of these species may be partially accounted for by the fact that the oxidation of the isomeric 2,4-hexadiene mixture (which is likely to contain contributions from trans,trans, trans,cis, and cis,cis isomers) will generate both *trans*- and *cis*-crotonaldehyde (although the trans isomer might be expected to make the greater contribution on the basis of stability considerations). The observed yield of *trans*-crotonaldehyde is therefore a lower limit for the total yield of the crotonaldehyde isomers.

There are a number of mechanistic reasons that could contribute to the observed yields of both acetaldehyde and crotonaldehyde being lower than predicted. For example, the assumption that the addition of O_2 to the resonance-stabilized 2-hydroxyhexenyl radical occurs with equal probability at the two possible positions could be erroneous. If the 2,5 sequential addition of OH and O_2 is significantly favored over the 2,3

addition, a greater yield of 5-hydroxy-3-hexen-2-one would be expected, at the expense of acetaldehyde and crotonaldehyde.

Other possible factors relate to the existence of alternative mechanistic pathways, which are not represented in Figure 3, and two such possibilities have been considered. First, the cis isomer of the 2-hydroxy-4-hexenyl-3-oxy radical could undergo a competitive 1,5 H atom shift isomerization to generate a resonance-stabilized 2,3-dihydroxyhexenyl radical:

$$CH_3CH(OH)CH(O)CH{=}CHCH_3 \rightarrow CH_3CH(OH)CH(OH)CH{=}CH\dot{C}H_2 \leftrightarrow CH_3CH(OH)CH(OH)\dot{C}HCH{=}CH_2 \quad (12)$$

The subsequent addition of O_2 to generate the secondary peroxy radical, $CH_3CH(OH)CH(OH)CH(O_2)CH{=}CH_2$, would be expected to dominate, since the other peroxy radical would be primary. This initiates a sequence of reactions, involving decomposition of the corresponding β-hydroxy oxy radical, which are likely to generate acrolein ($CH_2{=}CHCHO$) as follows:

$$CH_3CH(OH)CH(OH)CH(O_2)CH{=}CH_2 + NO \rightarrow CH_3CH(OH)CH(OH)CH(O)CH{=}CH_2 + NO_2 \quad (13)$$

$$CH_3CH(OH)CH(OH)CH(O)CH{=}CH_2 \rightarrow CH_3CH(OH)\dot{C}H(OH) + CH_2{=}CHCHO \quad (14)$$

$$CH_3CH(OH)\dot{C}H(OH) + O_2 \rightarrow CH_3CH(OH)CHO + HO_2 \quad (15)$$

Acrolein was detected as a minor product, with a molar yield of ca. 1−3%, providing some support for the minor contribution of 1,5-isomerization to the fate of the *cis*-**2**-hydroxy-4-hexenyl-3-oxy radical.

Another factor that potentially contributes to the low yields of both acetaldehyde and crotonaldehyde relates to their partial formation from reactions of O_2 with the corresponding α-hydroxy radicals $CH_3\dot{C}HOH$ and $CH_3C{=}CH\dot{C}HOH$, following the decomposition of the 2-hydroxy-4-hexenyl-3-oxy and 3-hydroxy-4-hexenyl-2-oxy radicals (see Figure 3), e.g., in the case of $CH_3\dot{C}HOH$:

$$CH_3\dot{C}HOH + O_2 \rightarrow CH_3CHO + HO_2 \quad (16)$$

The mechanism of this class of reaction has been the subject of some debate,[27−30] but at room temperature, it is generally accepted to involve the isomerization and decomposition of an intermediate peroxy radical:

$$CH_3\dot{C}HOH + O_2 \rightarrow CH_3CH(OH)O_2 \rightarrow CH_3CH(O)OOH \rightarrow CH_3CHO + HO_2 \quad (16')$$

An isomerization−decomposition rate of ca. 100 s^{-1} has been estimated for $CH_3CH(OH)O_2$[31] formed from the reverse reaction of CH_3CHO with HO_2, and a value of 100 ± 50 s^{-1} at 295 K has been reported for the related α-hydroxy peroxy radical $HOCH_2O_2$[32] formed from the reaction of HCHO with HO_2. If a similar rate is assumed for $CH_3CH{=}CHCH(OH)O_2$ in the 2,4-hexadiene system, it is possible that the reactions with NO can compete under the conditions of the present study. Assuming a rate coefficient for reaction with NO of 8.5×10^{-12} cm^3 $molecule^{-1}$ s^{-1} (i.e., typical of those reported for RO_2 radicals[33]), millitorr concentrations of NO are sufficient for this reaction to be favored. The reactions of $CH_3CH(OH)O_2$ and $CH_3CH{=}CHCH(OH)O_2$ with NO would be expected to lead to the generation of acetic and crotonic acids, e.g., for $CH_3CH(OH)O_2$

$$CH_3CH(OH)O_2 + NO \rightarrow CH_3CH(OH)O + NO_2 \quad (17)$$

$$CH_3CH(OH)O + O_2 \rightarrow CH_3C(O)OH + HO_2 \quad (18)$$

thereby lowering the yields of both acetaldehyde and crotonaldehyde. If reaction 17, and the corresponding reaction for $CH_3CH{=}CHCH(OH)O_2$, are assumed to be exclusive, then molar yields of acetaldehyde and crotonaldehyde of approximately 30% and 20%, respectively, would be predicted. This adjusted predicted yield for acetaldehyde is in agreement with that observed, and that for crotonaldehyde is consistent with the lower limit derived from observation of the trans isomer. However, infrared features attributable to acetic acid were not observable, and an upper limit of 2% for the molar yield of this species was derived. A calibrated reference spectrum for crotonic acid was not available. It therefore appears that the removal of $CH_3CH(OH)O_2$ and $CH_3CH{=}CHCH(OH)O_2$ by reaction with NO is not important in this system, unless products other than the acids are generated. It is not therefore possible to account fully for the observed low yields of acetaldehyde and crotonaldehyde, or for their nonequivalence, although some of the above factors may contribute.

The minor abstraction of hydrogen from the terminal CH_3-groups (not shown in Figure 3) generates a superallyl radical that may be represented by three canonical forms:

$$CH_3CH{=}CHCH{=}CH\dot{C}H_2 \leftrightarrow CH_3CH{=}CH\dot{C}HCH{=}CH_2 \leftrightarrow CH_3\dot{C}HCH{=}CHCH{=}CH_2 \quad (19)$$

Subsequent addition of O_2 to form the secondary peroxy radical, $CH_3CH(O_2)CH{=}CHCH{=}CH_2$, would be expected to dominate, since addition of O_2 at the other possible positions forms either a primary peroxy radical or a secondary peroxy radical in which the diene conjugation is lost. It is likely that the subsequent chemistry, via the corresponding oxy radical, will lead mainly to the formation of 3,5-hexadien-2-one.

3.3. Kinetics of the Reactions of NO_2 with 2,4-Hexadiene and 1,3-Butadiene. The kinetics of reactions 8 and 10 were studied by monitoring the loss of 2,4-hexadiene and 1,3-butadiene in the presence of excess NO_2:

$$NO_2 + \text{2,4-hexadiene} \rightarrow \text{products} \quad (8)$$

$$NO_2 + \text{1,3-butadiene} \rightarrow \text{products} \quad (10)$$

Initial reactant concentrations were 15−300 mTorr of NO_2 and 2−12 mTorr of either 2,4-hexadiene or 1,3-butadiene in 700 Torr of air, O_2, or N_2 diluent. NO_2 was always in large excess, and as shown in the insets in Figures 4 and 5, the observed loss of 2,4-hexadiene and 1,3-butadiene followed pseudo-first-order kinetics. Figures 4 and 5 show plots of the observed pseudo-first-order loss rates of 2,4-hexadiene and 1,3-butadiene as a function of the NO_2 concentration in the chamber. As seen in Figure 4, there was no discernible difference between the kinetic data obtained in either O_2 or N_2 diluent. Linear least-squares analyses of the data in Figures 4 and 5 give second-order rate constants $k_8 = (3.11 \pm 0.18) \times 10^{-19}$ cm^3 $molecule^{-1}$ s^{-1} and $k_{10} = (2.54 \pm 0.15) \times 10^{-20}$ cm^3 $molecule^{-1}$ s^{-1}. Quoted errors are two standard deviations from the regression analysis.

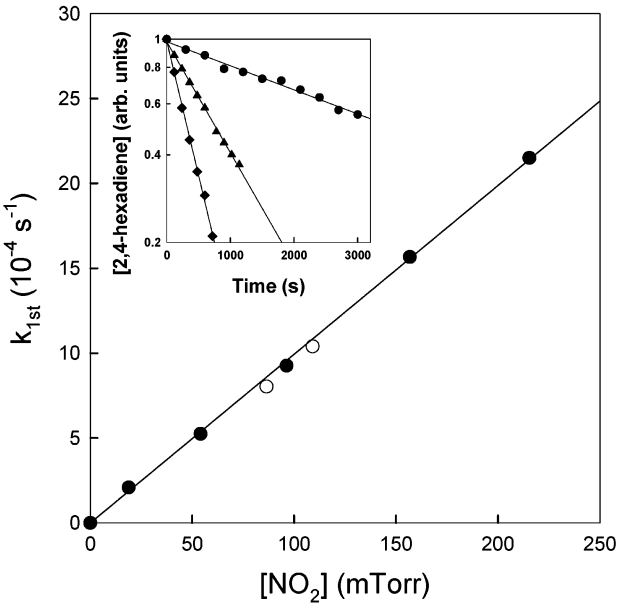

Figure 4. Pseudo first-order loss rate of 2,4-hexadiene versus NO_2 concentration observed in 2,4-hexadiene/NO_2 mixtures in 700 Torr of either O_2 (●) or N_2 (○) diluent. The inset shows representative decays of 2,4-hexadiene in the presence of either 25 (●), 92 (▲), or 187 (◆) mTorr of NO_2.

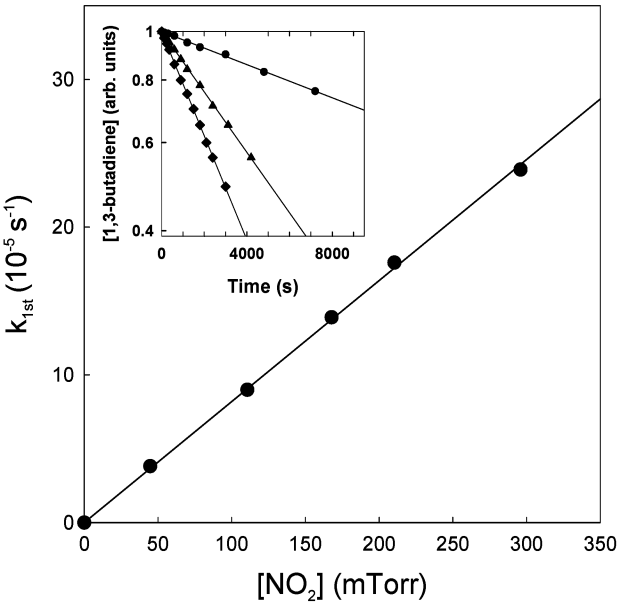

Figure 5. Pseudo-first-order loss rate of 1,3-butadiene versus NO_2 concentration observed in 2,4-hexadiene/NO_2 mixtures in 700 Torr of air diluent. The inset shows representative decays of 1,3-butadiene in the presence of either 45 (●), 168 (▲), or 296 (◆) mTorr of NO_2.

The measurement of k_8 reported herein is approximately a factor of 2 lower than the values of $k_8 = (5.4 \pm 0.8) \times 10^{-19}$ and $(5.9 \pm 0.9) \times 10^{-19}$ cm^3 molecule^{-1} s^{-1} reported by Ohta et al.[34] for the cis,trans and trans,trans isomers of 2,4-hexadiene, respectively. Ohta et al. measured k_8 relative to the reaction of NO_2 with isoprene. The value for $k_{(NO_2+isoprene)} = 1.8 \times 10^{-19}$ cm^3 molecule^{-1} s^{-1} used by Ohta et al. to place their relative rate data on an absolute basis is substantially higher than the values of 1.16×10^{-19} cm^3 molecule^{-1} s^{-1}, reported by Glasson and Tuesday,[35] and 1.03×10^{-19} cm^3 molecule^{-1} s^{-1}, reported by Atkinson et al.[7] Use of an average of these values, $k_{(NO_2+isoprene)} = 1.1 \times 10^{-19}$, to scale the relative rate data of Ohta et al. gives $k_8 = (3.3 \pm 0.5) \times 10^{-19}$ and $(3.6 \pm 0.6) \times 10^{-19}$ cm^3 molecule^{-1} s^{-1} for the cis,trans and trans,trans isomers, entirely consistent with the results from the present work. We conclude that the measurement of $k_{(NO_2+isoprene)} = 1.8 \times 10^{-19}$ by Ohta et al.[34] is in error and their relative rate data should be rescaled relative to $k_{(NO_2+isoprene)} = 1.1 \times 10^{-19}$ cm^3 molecule^{-1} s^{-1}.

Our value for $k_{10} = (2.54 \pm 0.15) \times 10^{-20}$ can be compared with previous determinations of $k_{10} = (2.86 \pm 0.09) \times 10^{-20}$ cm^3 molecule^{-1} s^{-1} [35] and $(3.1 \pm 0.3) \times 10^{-20}$ cm^3 molecule^{-1} s^{-1}.[7] Our result is slightly lower than these previous determinations. Similar techniques (measurement of pseudo-first-order loss of 1,3-butadiene in the presence of a large excess of NO_2) were used in the three different studies. In view of the simplicity of the measurements, it is surprising that the results from the various studies are not in better agreement.

The available trends in the kinetics database for reactions of NO_2 with alkenes and dienes[6,10] indicate that the reactions occur by an addition mechanism and provide an insight into the likely distribution of radicals initially generated from the reaction of NO_2 with 2,4-hexadiene. As discussed by Ohta et al.,[34] the significantly higher reactivity of conjugated dienes, compared with monoalkenes or unconjugated dienes, suggests that addition of NO_2 to generate the resonance-stabilized nitroalkenyl radical is favored, e.g.

$$NO_2 + \text{2,4-hexadiene} \rightarrow CH_3CH(NO_2)\dot{C}HCH{=}CHCH_3 \leftrightarrow CH_3CH(NO_2)CH{=}CH\dot{C}HCH_3 \quad (8)$$

This also allows the unpaired electron to be located remotely (i.e.,at the δ position) from the deactivating influence of the -NO_2 group. The substantially higher reactivity of 2,4-hexadiene compared with 1,3-butadiene may therefore reflect the fact that the δ-substituted location is secondary in the 2,4-hexadiene system and therefore significantly more stabilized than the corresponding primary radical formed in the 1,3-butadiene system. It seems likely, therefore, that the subsequent reactions of the nitrohexenyl radical proceed via addition (e.g., of O_2) at the position δ to the NO_2 group, and this is assumed in the mechanistic appraisal in the following sections.

The reactivity of 2,4-hexadiene with NO was also investigated. No discernible reaction was detected over a period of 1 h in a mixture of 26 mTorr of 2,4-hexadiene and 100 mTorr of NO in 700 Torr of N_2 diluent. The experiment was repeated with a low concentration (1 Torr) of O_2 also present. Again, no detectable decay of 2,4-hexadiene concentration was observed until low concentrations of NO_2 were generated in the system by the reaction

$$NO + NO + O_2 \rightarrow NO_2 + NO_2 \quad (20)$$

On the basis of these observations, we derive an upper limit value of $k \leq 2 \times 10^{-21}$ cm^3 molecule^{-1} s^{-1} for the reaction of NO with 2,4-hexadiene.

3.4. Mechanism of the Reaction of NO_2 with 2,4-Hexadiene. *3.4.1. Experiments in N_2 Diluent.*. The relative removal of NO_2 and 2,4-hexadiene in 700 Torr of N_2 diluent was investigated under conditions when neither reagent was present in large excess. The results, shown in Figure 6, indicate removal of 1.98 ± 0.07 molecules of NO_2 for every 2,4-hexadiene molecule removed, which is consistent with a mechanism involving the sequential addition of two NO_2 molecules to 2,4-hexadiene, predominantly yielding the 2,5-dinitro-substituted hexene, $CH_3CH(NO_2)CH{=}CHCH(NO_2)CH_3$. Consistent with

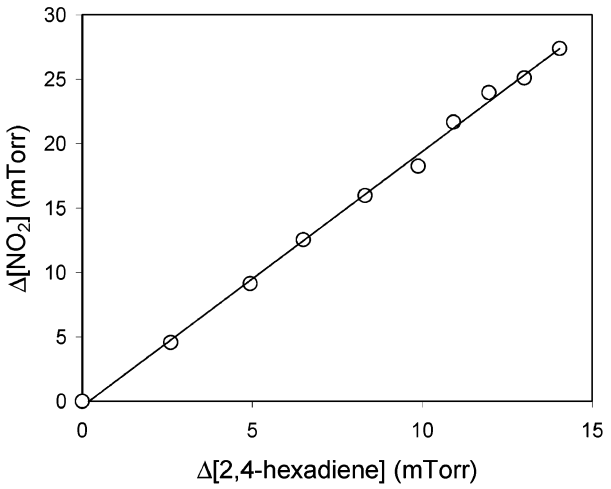

Figure 6. Observed relative loss of NO_2 and 2,4-hexadiene in 700 Torr of N_2 diluent. Line is linear regression of the data: $\Delta[NO_2] = (1.98 \pm 0.07)\Delta[2,4\text{-hexadiene}] - (0.39 \pm 0.64)$, where quoted errors are two standard deviations.

this, FTIR product features were observed at 774, 1360, 1390, and 1679 cm^{-1}. The 774 cm^{-1} feature can be assigned to an NO_2 scissors mode, and the features at 1360 and 1390 cm^{-1} can be attributed to CH_3 deformations. The feature at 1679 cm^{-1} can be assigned to either a *trans*-C=C stretch (the corresponding cis isomer feature would be expected at 1645−1665 cm^{-1}, where absorption by NO_2 reagent precludes reliable measurements) or an NO_2 asymmetric stretch, or both. Nitrous acid (HONO) was not detected as a product, indicating that its yield is <0.5%. This confirms that H-atom abstraction makes no significant contribution to the reaction of NO_2 with 2,4-hexadiene.

3.4.2. Experiments in O_2 Diluent. The relative removal of NO_2 and 2,4-hexadiene was also investigated in a series of experiments in 700 Torr of O_2 diluent. The results, shown in Figure 7, indicate that in the early stages of each experiment two molecules of NO_2 were consumed for every 2,4-hexadiene molecule, while at longer extents of reaction, the stoichiometry decreased to significantly less than 2. The initial removal of two NO_2 molecules is interpreted in terms of the formation of a nitrohexenylperoxynitrate, by the following reaction sequence:

$$NO_2 + \text{2,4-hexadiene} \rightarrow CH_3CH(NO_2)CH{=}CH\dot{C}HCH_3 \quad (8')$$

$$CH_3CH(NO_2)CH{=}CH\dot{C}HCH_3 + O_2 \rightarrow CH_3CH(NO_2)CH{=}CHCH(O_2)CH_3 \quad (21)$$

$$CH_3CH(NO_2)CH{=}CHCH(O_2)CH_3 + NO_2 \rightleftarrows CH_3CH(NO_2)CH{=}CHCH(O_2NO_2)CH_3 \quad (22,-22)$$

FTIR product features at 791, 1046, 1155, 1296, 1360, 1389, and 1719 cm^{-1} are consistent with the formation of $CH_3CH(NO_2)CH{=}CHCH(O_2NO_2)CH_3$. The 791, 1296, and 1719 cm^{-1} features can be assigned to NO_2 scissors, NO_2 symmetric stretch, and NO_2 asymmetric stretching modes, while the features at 1360 and 1389 cm^{-1} can be attributed to CH_3 deformations.

The peroxynitrate is expected to be rapidly equilibrated with the peroxy radical. At greater extents of reaction, therefore, the slow removal of the peroxy radical by its self-reaction leads to the progressive loss of the nitrohexenylperoxynitrate and the generation of alternative organic products, most of which contain

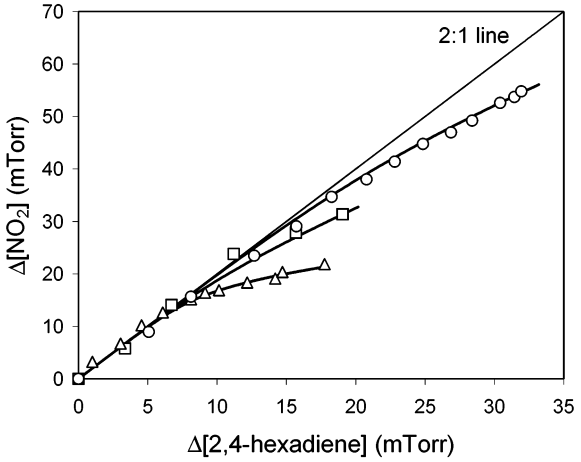

Figure 7. Observed relative loss of NO_2 and 2,4-hexadiene in 700 Torr of O_2 diluent. Initial concentrations of NO_2 were 112 mTorr (○), 58 mTorr (□), and 25 mTorr (△). Initial concentration of ca. 50 mTorr of 2,4-hexadiene were used in all experiments. Curved lines are simulations with an assumed mechanism (see text).

only one oxidized nitrogen group:

$$2CH_3CH(NO_2)CH{=}CHCH(O_2)CH_3 \rightarrow 2CH_3CH(NO_2)CH{=}CHCH(O)CH_3 \quad (23a)$$

$$\rightarrow CH_3CH(NO_2)CH{=}CHCH(OH)CH_3 + CH_3CH(NO_2)CH{=}CHC(O)CH_3 + O_2 \quad (23b)$$

On the basis of the products typically observed from the self-reactions of peroxy radicals (e.g., Lesclaux[36]), the reaction is expected to generate both nitrohexenyl alcohol and ketone products via a terminating reaction (eq 23b) and the corresponding oxy radical via a propagating reaction (eq 23a). Under the experimental conditions, the oxy radical would be expected to react either with O_2 (providing another route to the nitrohexenyl ketone) or with NO_2 to form a nitrohexenyl nitrate:

$$CH_3CH(NO_2)CH{=}CHCH(O)CH_3 + O_2 \rightarrow CH_3CH(NO_2)CH{=}CHC(O)CH_3 + HO_2 \quad (24)$$

$$CH_3CH(NO_2)CH{=}CHCH(O)CH_3 + NO_2 \rightarrow CH_3CH(NO_2)CH{=}CHC(ONO_2)CH_3 \quad (25)$$

Reaction 24 also generates HO_2 radicals, which are mainly sequestered in the form of HO_2NO_2 under the conditions of these experiments:

$$HO_2 + NO_2 (+M) \rightleftarrows HO_2NO_2 (+M) \quad (26,-26)$$

HO_2NO_2 was identified as a product (see Figure 8), providing support for this mechanism and positively confirming the ultimate formation of HO_x radicals from the reaction of NO_2 with 2,4-hexadiene. The system was simulated on the basis of the reaction sequence discussed above (also shown in Table 1) by use of the FACSIMILE kinetics integration package (UES Software, 2000). As shown in Figure 8, the time dependences of 2,4-hexadiene and NO_2 were well described with an equilibrium coefficient for reaction 22 of $K_{22} = 2.1 \times 10^{-12}$ cm^3 $molecule^{-1}$ ($k_{22} = 7.5 \times 10^{-12}$ cm^3 $molecule^{-1}$ s^{-1}; $k_{-22} = 3.5$ s^{-1}) and a self-reaction rate coefficient $k_{23} = 3.3 \times 10^{-12}$ cm^3 $molecule^{-1}$ s^{-1}. The values of k_{22} and k_{-22} are close to those reported for alkyl peroxy radicals such as $C_2H_5O_2$,[37] and the value of k_{23} is based on those reported for hydroxy-substituted

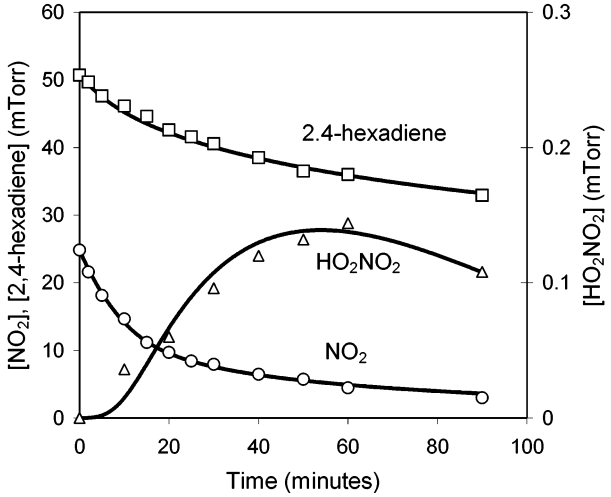

Figure 8. Time dependence of NO_2 and 2,4-hexadiene in experiment performed in 700 Torr of O_2 diluent. Lines are simulations with the mechanism and parameters in Table 1 (see text).

peroxy radicals formed in diene systems.[22] Although these parameter values are entirely reasonable, they do not uniquely describe the profiles of 2,4-hexadiene and NO_2 in Figure 8; however, it was clear that both decomposition of the peroxynitrate and the self-reaction of the associated peroxy radical have to be comparatively rapid to provide a good description of the data in Figures 7 and 8. At the end of the experiment presented in Figure 8, the peroxynitrate is calculated to make only a minor contribution to the organic oxidized nitrogen species, and the overall removal stoichiometry, $\Delta[NO_2]/\Delta$[2,4-hexadiene], is 1.24.

The observed low concentrations of HO_2NO_2 (Figure 8) are consistent with only a very small fraction (ca. 2%) of reaction 23 proceeding via route a. The gradual decrease in the concentration of HO_2NO_2 in the latter stages of the experiment results from its equilibration with HO_2 and NO_2 in reaction 26, the slow removal of HO_2 by its self-reaction and reaction with nitrohexenyl peroxy radicals, and the steady decay of NO_2. As shown in Figure 8, the reaction mechanism used in these simulations provides a good description of the observed time dependence of HO_2NO_2 throughout the experiment.

3.4.3. Experiments in the Presence of NO and O_2. The system was further investigated in a series of experiments in which NO was also present. The initial conditions of the experiments are given in Table 2. The main objective of these experiments was to look for evidence of additional HO_x-catalyzed removal of 2,4-hexadiene when NO is present, resulting from the formation of HO_2 from the NO_2-initiated chemistry, as illustrated schematically in Figure 9. In the presence of NO, efficient conversion of the nitrohexenylperoxy radical to the corresponding oxy radical occurs via reaction 27a, with some simultaneous radical termination occurring via reaction 27b:

$$CH_3CH(NO_2)CH{=}CHCH(O_2)CH_3 + NO \rightarrow CH_3CH(NO_2)CH{=}CHCH(O)CH_3 + NO_2 \quad (27a)$$

$$\rightarrow CH_3CH(NO_2)CH{=}CHCH(ONO_2)CH_3 \quad (27b)$$

These reactions preclude the buildup of the nitrohexenylperoxy nitrate observed in the absence of NO and also provide the potential for significant generation of HO_x radicals from the subsequent reaction (eq 24) of the oxy radical, $CH_3CH(NO_2)CH{=}CHCH(O)CH_3$.

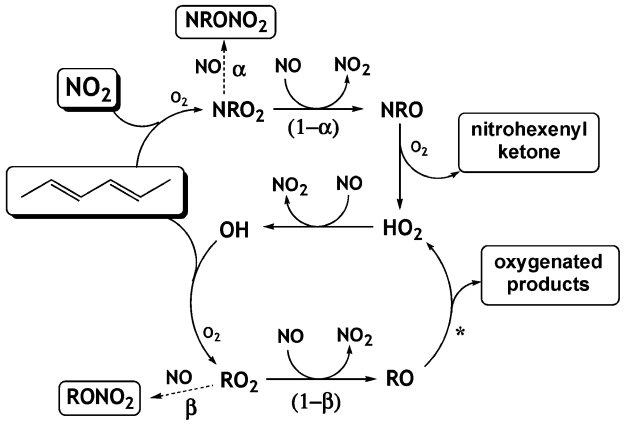

Figure 9. Schematic representation of the salient mechanistic features of NO_2-initiated oxidation of 2,4-hexadiene in the presence of NO and O_2. The initial sequence leads to partial formation of HO_x radicals and supplementary catalytic loss of 2,4-hexadiene via reaction with OH radicals. The mechanism also promotes NO-to-NO_2 conversion and is therefore autocatalytic. NR represents the nitrohexenyl group in radicals generated from the NO_2-initiated oxidation. R is a collective representation of the organic groups (R1−R4) in radicals generated from the OH-initiated oxidation. Structures are given in footnote *a* of Table 1. Conversion of RO to HO_2 (*) occurs by a variety of pathways, as shown in Figure 3.

Because this chemistry converts NO to NO_2, initial concentrations of NO_2 were arranged to be at or close to zero. Even when initially zero, some formation of NO_2 occurs from the reaction

$$NO + NO + O_2 \rightarrow NO_2 + NO_2 \quad (20)$$

allowing the chemistry in Figure 9 to be initiated.

The time dependence of NO, NO_2, and 2,4-hexadiene in one experiment is shown in Figure 10, which is typical of that observed in all experiments in 700 Torr of O_2 diluent. The progressive conversion of NO to NO_2 is accompanied by decay of 2,4-hexadiene, which is due to its removal by reaction with both NO_2 and OH. On the basis of the measured NO_2 concentrations and the value of k_8 reported above in section 3.3, the observed decay rate of 2,4-hexadiene was consistent with between ca. 58% and 74% of its removal being due to reaction with OH in these experiments (see Table 2). Consistent with this, acetaldehyde, crotonaldehyde, and 2,5-dimethylfuran were observed as products, with yields that were (65 ± 6)% of those observed from the OH-initiated chemistry (section 3.2), based on the results of experiments A−E in Table 2.

Once NO is consumed, the removal rate of 2,4-hexadiene decreases, and the system reverts to that described above in section 3.4.2 with concentrations of both 2,4-hexadiene and NO_2 decreasing. The contrast between the behavior of the system in the presence and absence of NO is further illustrated in Figure 11. When NO is present, the removal stoichiometry, $\Delta[NO_x]/\Delta$[2,4-hexadiene], is significantly below unity. Once NO is consumed, a value between 1 and 2 is observed, consistent with the results presented in section 3.4.2.

As illustrated in Figure 9, the major termination steps when NO is present are likely to be formation of the nitrohexenyl nitrate (reaction 7b) and the analogous formation of nitrates from the reactions of the peroxy radicals generated from the OH-initiated chemistry (reaction 11b). Making the assumption that these reactions alone are responsible for radical termination in the presence of NO, and denoting the branching ratio k_{27b}/k_{27} as α and k_{11b}/k_{11} as β, the loss of 2,4-hexadiene for every

TABLE 1: Reactions and Kinetic Parameters Used To Simulate the NO_2-Initiated Chemistry

reaction[a]			branching ratio	rate or equilibrium coefficient[b]	comment
		NO_2-Initiated Reactions			
2,4-hexadiene + NO_2	→	NRO_2		3.11×10^{-19}	*c*
NRO_2 + NO	→	NRO + NO_2	$1-\alpha$	8.6×10^{-12}	*d, e*
	→	$NRONO_2$	α		
NRO_2 + NO_2	⇄	NRO_2NO_2		2.1×10^{-12} cm^3 molecule^{-1}	*f*
NRO_2 + HO_2	→	NROOH + O_2		1.8×10^{-11}	*d*
NRO + O_2	→	$CH_3CH(NO_2)CH{=}CHC(O)CH_3$ + HO_2		7.6×10^{-15}	*g*
NRO + NO	→	NRONO, or NO_2 + NO_2 + organic product(s)		3.8×10^{-11}	*g*
NRO + NO_2	→	$NRONO_2$		3.8×10^{-11}	*g*
		OH-Initiated Reactions			
2,4-hexadiene + OH	→	$R1O_2$	0.426	1.76×10^{-10}	*c, e*
2,4-hexadiene + OH	→	$R2O_2$	0.270		
2,4-hexadiene + OH	→	$R3O_2$	0.270		
2,4-hexadiene + OH	→	$R4O_2$	0.034		
$R1O_2$ + NO	→	R1O + NO_2	$1-\beta$	8.6×10^{-12}	*d, e*
	→	$R1ONO_2$	β		
$R1O_2$ + NO_2	⇄	$R1O_2NO_2$		2.1×10^{-12} cm^3 molecule^{-1}	*f, h*
$R1O_2$ + HO_2	→	R1OOH + O_2		1.8×10^{-11}	*d*
R1O → →	→	2,5-dimethylfuran + HO_2 (0.165)	0.165	2.0×10^{6} s^{-1}	*i, e*
	→	CH_3CHO + $CH_3CH{=}CHOH$ (0.835)	0.835		
R1O + NO	→	R1ONO		3.8×10^{-11}	*g*
R1O + NO_2	→	$R1ONO_2$		3.8×10^{-11}	*g*
$CH_3CH{=}CHOH$ + O_2	→	$CH_3CH{=}CHO$ + HO_2		1.9×10^{-11}	*j, k*
$R2O_2$ + NO	→	R2O + NO_2	$1-\beta$	8.6×10^{-12}	*d, e*
	→	$R2ONO_2$	β		
$R2O_2$ + NO_2	⇄	$R2O_2NO_2$		2.1×10^{-12} cm^3 molecule^{-1}	*f, h*
$R2O_2$ + HO_2	→	R2OOH + O_2		1.8×10^{-11}	*d*
R2O	→	$CH_3CH{=}CHO$ + CH_3CHOH		2.0×10^{6} s^{-1}	*i*
R2O + NO	→	R2ONO		3.8×10^{-11}	*g*
R2O + NO_2	→	$R2ONO_2$		3.8×10^{-11}	*g*
CH_3CHOH + O_2	→	CH_3CHO + HO_2		1.9×10^{-11}	*j*
$R3O_2$ + NO	→	R3O + NO_2	$1-\beta$	8.6×10^{-12}	*d, e*
	→	$R3ONO_2$	β		
$R3O_2$ + NO_2	⇄	$R3O_2NO_2$		2.1×10^{-12} cm^3 molecule^{-1}	*f, h*
$R3O_2$ + HO_2	→	R3OOH + O_2		1.8×10^{-11}	*d*
R3O + O_2	→	$CH_3CH(OH)CH{=}CHC(O)CH_3$ + HO_2		7.6×10^{-15}	*g*
R3O + NO	→	R3ONO		3.8×10^{-11}	*g*
R3O + NO_2	→	$R3ONO_2$		3.8×10^{-11}	*g*
$R4O_2$ + NO	→	R4O + NO_2	$1-\beta$	8.6×10^{-12}	*d, e*
	→	$R4ONO_2$	β		
$R4O_2$ + NO_2	⇄	$R4O_2NO_2$		2.1×10^{-12} cm^3 molecule^{-1}	*f, h*
$R4O_2$ + HO_2	→	R4OOH + O_2		1.8×10^{-11}	*d*
R4O + O_2	→	$CH_2{=}CHCH{=}CHC(O)CH_3$ + HO_2		7.6×10^{-15}	*g*
R4O + NO	→	R4ONO		3.8×10^{-11}	*g*
R4O + NO_2	→	$R4ONO_2$		3.8×10^{-11}	*g*
		Peroxy Radical Self-Reactions			
NRO_2 + NRO_2	→	NRO + NRO + O_2	0.02	3.34×10^{-12}	*l, m*
	→	NROH + $CH_3CH(NO_2)CH{=}CHC(O)CH_3$ + O_2	0.98		
$R1O_2$ + $R1O_2$	→	R1O + R1O + O_2	0.8	5.74×10^{-12}	*l*
	→	R1OH + $CH_3C(O)CH(OH)CH{=}CHCH_3$ + O_2	0.2		
$R2O_2$ + $R2O_2$	→	R2O + R2O + O_2	0.8	5.74×10^{-12}	*l*
	→	R2OH + $CH_3CH(OH)C(O)CH{=}CHCH_3$ + O_2	0.2		
$R3O_2$ + $R3O_2$	→	R3O + R3O + O_2	0.8	3.34×10^{-12}	*l*
	→	R3OH + $CH_3CH(OH)CH{=}CHC(O)CH_3$ + O_2	0.2		
	→	$R4O_2$ + $R4O_2$ R4O + R4O + O_2	0.8	4.75×10^{-13}	*l*
	→	R4OH + $CH_2{=}CHCH{=}CHC(O)CH_3$ + O_2	0.2		
		Peroxy Radical Cross Reactions			
NRO_2 + $R1O_2$	→	NRO + R1O + O_2	0.8	4.38×10^{-12}	*l, n*
	→	NROH + $CH_3C(O)CH(OH)CH{=}CHCH_3$ + O_2	0.1		
	→	R1OH + $CH_3CH(NO_2)CH{=}CHC(O)CH_3$ + O_2	0.1		
NRO_2 + $R2O_2$	→	NRO + R2O + O_2	0.8	1.65×10^{-12}	*l, n*
	→	NROH + $CH_3CH(OH)C(O)CH{=}CHCH_3$ + O_2	0.1		
	→	R2OH + $CH_3CH(NO_2)CH{=}CHC(O)CH_3$ + O_2	0.1		
NRO_2 + $R3O_2$	→	NRO + R3O + O_2	0.8	3.34×10^{-12}	*l, n*
	→	NROH + $CH_3CH(OH)CH{=}CHC(O)CH_3$ + O_2	0.1		
	→	R3OH + $CH_3CH(NO_2)CH{=}CHC(O)CH_3$ + O_2	0.1		
NRO_2 + $R4O_2$	→	NRO + R4O + O_2	0.8	1.26×10^{-12}	*l, n*
	→	NROH + $CH_2{=}CHCH{=}CHC(O)CH_3$ + O_2	0.1		
	→	R4OH + $CH_3CH(NO_2)CH{=}CHC(O)CH_3$ + O_2	0.1		

TABLE 1 (Continued)

reaction[a]			branching ratio	rate or equilibrium coefficient[b]	comment
$R1O_2 + R2O_2$	→	$R1O + R2O + O_2$	0.8	5.74×10^{-12}	*l*
	→	$R1OH + CH_3CH(OH)C(O)CH{=}CHCH_3 + O_2$	0.1		
	→	$R2OH + CH_3C(O)CH(OH)CH{=}CHCH_3 + O_2$	0.1		
$R1O_2 + R3O_2$	→	$R1O + R3O + O_2$	0.8	4.38×10^{-12}	*l*
	→	$R1OH + CH_3CH(OH)CH{=}CHC(O)CH_3 + O_2$	0.1		
	→	$R3OH + CH_3C(O)CH(OH)CH{=}CHCH_3 + O_2$	0.1		
$R1O_2 + R4O_2$	→	$R1O + R4O + O_2$	0.8	4.38×10^{-12}	*l*
	→	$R1OH + CH_2{=}CHCH{=}CHC(O)CH_3 + O_2$	0.1		
	→	$R4OH + CH_3C(O)CH(OH)CH{=}CHCH_3 + O_2$	0.1		
$R2O_2 + R3O_2$	→	$R2O + R3O + O_2$	0.8	1.65×10^{-12}	*l*
	→	$R2OH + CH_3CH(OH)CH{=}CHC(O)CH_3 + O_2$	0.1		
	→	$R3OH + CH_3CH(OH)C(O)CH{=}CHCH_3 + O_2$	0.1		
$R2O_2 + R4O_2$	→	$R2O + R4O + O_2$	0.8	1.65×10^{-12}	*l*
	→	$R2OH + CH_2{=}CHCH{=}CHC(O)CH_3 + O_2$	0.1		
	→	$R4OH + CH_3CH(OH)C(O)CH{=}CHCH_3 + O_2$	0.1		
$R3O_2 + R4O_2$	→	$R3O + R4O + O_2$	0.8	1.26×10^{-12}	*l*
	→	$R3OH + CH_2{=}CHCH{=}CHC(O)CH_3 + O_2$	0.1		
	→	$R4OH + CH_3CH(OH)CH{=}CHC(O)CH_3 + O_2$	0.1		
		Inorganic Reactions			
$NO + NO + O_2$	→	$NO_2 + NO_2$		2.0×10^{-38} cm^6 molecule^{-2} s^{-1}	*j*
$HO_2 + NO$	→	$OH + NO_2$		9.0×10^{-12}	*j*
$HO_2 + NO_2$	⇄	HO_2NO_2		2.5×10^{-11} cm^3 molecule^{-1}	*j, o*
$HO_2 + HO$	→	$H_2O_2 + O_2$		2.9×10^{-12}	*j*
$OH + NO$	→	$HONO$		9.5×10^{-12}	*j*
$OH + NO_2$	→	HNO_3		1.1×10^{-11}	*j*

[a] NR, $CH_3CH(NO_2)\dot{C}H{=}CHCHCH_3$; R1, $CH_3\dot{C}HCH(OH)CH{=}CHCH_3$; R2, $CH_3\dot{C}H(OH)CHCH{=}CHCH_3$; R3, $CH_3CH(OH)CH{=}CH\dot{C}HCH_3$; R4, $CH_2{=}CHCH{=}CH\dot{C}HCH_3$. [b] 296 K, 700 Torr; units cm^3 molecule^{-1} s^{-1}, unless otherwise stated. [c] Rate coefficient determined in present study. [d] Saunders et al.[33] [e] See text for discussion of branching ratio. [f] 7.5×10^{-12} cm^3 molecule^{-1} s^{-1} and 3.53 s^{-1} used for forward and reverse reactions (see section 3.4.2). [g] Generic recommendation of Atkinson.[26] [h] Assumed equivalent to reaction of NRO_2. [i] Typical decomposition rate for β-hydroxyalkoxy radical.[26] [j] Atkinson et al.[37] [k] Assumed equivalent to reaction of $CH_3\dot{C}OH$. [l] Based on data of Jenkin et al.[22] for structurally similar radicals. [m] Rate coefficient assumed equivalent to OH-substituted analogue; branching ratios assigned on the basis of experimental data (see section 3.4.2). [n] Coefficients for nitro-substituted radical assumed equivalent to OH-substituted analogue. [o] Rate coefficients 1.4×10^{-12} cm^3 molecule^{-1} s^{-1} and 5.7×10^{-2} s^{-1} for forward and reverse reactions.

TABLE 2: Experimental Conditions and Results from NO_2/2,4-Hexadiene/NO/O_2 Experiments (296 K, 700 Torr)

run	$[NO]_0$ (mTorr)	$[NO_2]_0$ (mTorr)	[hexadiene]$_0$ (mTorr)	$[O_2]$ (Torr)	fractional removal by OH[a]	α, β[b]
A	2.2	0.00	4.6	700	0.74 ± 0.01	0.251
B	5.1	0.10	8.1	700	0.71 ± 0.01	0.246
C	12.4	0.45	16.2	700	0.66 ± 0.02	0.258
D	15.7	2.19	50.9	700	0.65 ± 0.02	0.253
E	38.5	3.54	51.0	700	0.58 ± 0.02	0.235
F	102.0	0.47	25.7	10[c]	0.00 ± 0.02	

[a] Determined from loss rate required to account for observed 2,4-hexadiene decay. [b] Optimized values from simulation of data with the mechanism in Table 1, assuming $\alpha = \beta$ (see text). [c] Balance N_2.

initiation event is given by

$$\Delta[\text{2,4-hexadiene}] = 1 + (1 - \alpha)/\beta \qquad \text{(i)}$$

where the first term represents loss by reaction with NO_2 and the second term represents loss by reaction with OH. The loss of NO_x for every initiation event is given by

$$\Delta[NO_x] = 2\alpha + (1 - \alpha) + (1 - \alpha) = 2 \qquad \text{(ii)}$$

where the respective terms represent loss as nitrohexenyl nitrate, nitrohexenyl ketone, and the various $RONO_2$ formed from reaction 11b. Combining eqs i and ii therefore suggests that the removal stoichiometry when NO is present is given by

$$\Delta[NO_x]/\Delta[\text{2,4-hexadiene}] = 2\beta/(1 - \alpha + \beta) \qquad \text{(iii)}$$

The data presented in Figure 11, for the experiments performed at the lowest NO_x, indicate that $\Delta[NO_x]/\Delta[\text{2,4-hexadiene}] = 0.52 \pm 0.06$, allowing a first indication of the values of α and β. In the absence of quantified yields of the nitrohexenyl nitrates formed from reaction 27b and the nitrates formed from reaction 11b, it is not possible to estimate α and β independently; however, making the assumption that $\alpha = \beta$ in eq iii provides a value of 0.26 ± 0.03 for each of the parameters. Reducing the value of one of the parameters leads to an increased value of the other to satisfy eq iii. For example, fixing β at a reduced value of 0.15 leads to a significantly elevated value of $\alpha =$

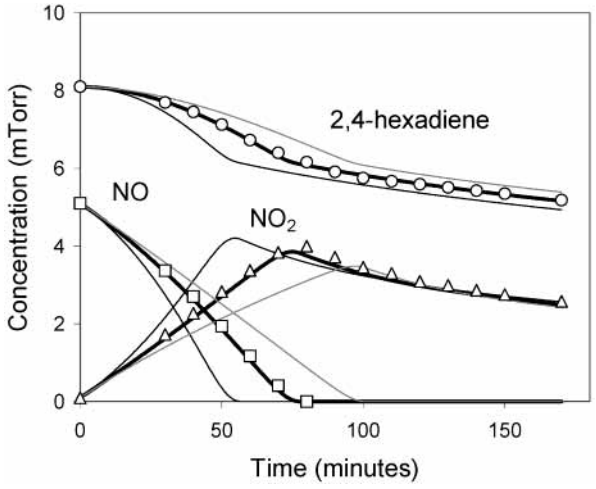

Figure 10. Time dependence of NO, NO_2, and 2,4-hexadiene in an experiment performed in 700 Torr of O_2 diluent (experiment B, Table 2). Lines are simulations with the mechanism in Table 1 (see text). Thick black line, $\alpha = \beta = 0.25$; thin black line, $\alpha = \beta = 0.15$; thin gray line, $\alpha = \beta = 0.35$.

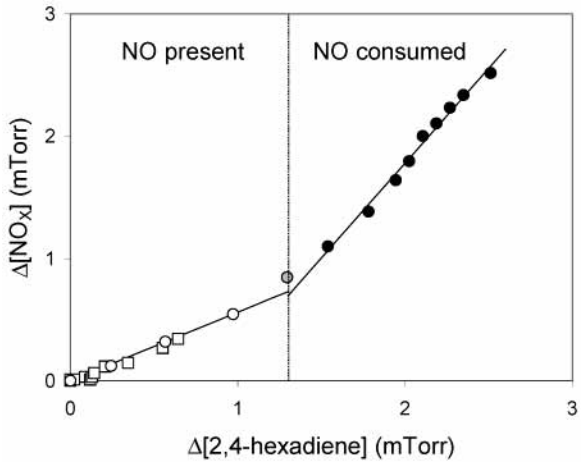

Figure 11. Observed relative loss of NO_x and 2,4-hexadiene during NO_2-initiated oxidation of 2,4-hexadiene, initially in the presence of NO (700 Torr of O_2 diluent). Data are shown for experiment B (circles) and for experiment A, "NO present" period only (squares). Regression analysis of "NO present" data (○, □) yields a slope of 0.52 ± 0.06. Regression analysis of "NO consumed" data (●) yields a slope of 1.55 ± 0.12. Quoted errors are two standard deviations.

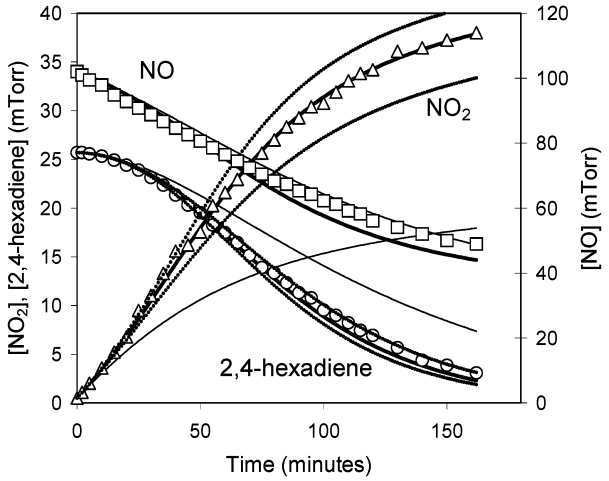

Figure 12. Time dependence of NO, NO_2, and 2,4-hexadiene in experiment performed with 10 Torr of O_2 (experiment F, Table 2). Lines are simulations based on the mechanism in Table 1 (see text). Thin solid lines: nitrohexenyloxy radical + NO reaction assumed to generate a nitrite product, $\alpha = 0.23$. Thick solid lines: nitrohexenyloxy radical + NO reaction assumed to generate 2 NO_2, $\alpha = 0.23$ (associated broken lines show results with α set at 0.15 and 0.35).

0.57, and reducing α to 0.15 leads to a slightly elevated value of $\beta = 0.30$.

In conjunction with eq i, any of the α, β pairs that satisfy eq iii indicate that 0.74 ± 0.03 of 2,4-hexadiene removal was due to reaction with OH when NO was present in the system. This is entirely consistent with that determined from the observed removal kinetics of 2,4-hexadiene in the lowest NO_x experiments (A and B), which form the basis of this analysis (see Table 2).

At increasing NO_x levels, the impact of reactions of some oxy radicals with NO and NO_2 has to be considered. On the basis of typical rate coefficients for these classes of reaction (e.g., Atkinson[26]), reactions with NO and NO_2 become significant (i.e., account for >5% of their removal) at $[O_2]/[NO_x] <$ ca. 10^5, for those oxy radicals that otherwise react with O_2. In particular, these reactions for the nitrohexenyloxy radical formed in the present system

$$CH_3CH(NO_2)CH{=}CHCH(O)CH_3 + NO_2 \rightarrow CH_3CH(NO_2)CH{=}CHC(ONO_2)CH_3 \quad (25)$$

$$CH_3CH(NO_2)CH{=}CHCH(O)CH_3 + NO \rightarrow \text{products} \quad (28)$$

reduce the efficiency of HO_x formation and therefore are almost certainly the main factor accounting for the gradual decrease in the contribution to 2,4-hexadiene removal made by reaction with OH as NO_x is increased (see Table 2). Accordingly, slightly higher values (up to ca. 0.7) were also observed for $\Delta[NO_x]/\Delta$[2,4-hexadiene] during the "NO present" period of the experiments performed with initial $[O_2]/[NO_x] < 10^5$ (experiments C−E, Table 2). To allow inclusion of these and other potentially competing reactions for peroxy and oxy radical intermediates, all experiments in Table 2 were therefore simulated by the chemical mechanism containing a detailed representation of the OH- and NO_2-initiated chemistry, which is listed in Table 1. The mechanism also includes associated inorganic chemical processes.

The simulated time profiles for NO, NO_2, and 2,4-hexadiene were optimized to the experimental data by varying the values of α and β, via nonlinear least-squares methodology, with the initial assumption that $\alpha = \beta$ (e.g., see Figure 10). The optimized values determined in each of the experiments (Table 2) are in good agreement, lying in the range 0.235−0.258, which is also consistent with the analytical solution based on the $\Delta[NO_x]/\Delta$[2,4-hexadiene] data presented above. Simulations with either α or β fixed at lower values yielded increased optimized values of the other parameter, which is also in broad agreement with the analytical solution.

The various optimized combinations of α and β provide simulated concentration−time traces for NO, NO_2, and 2,4-hexadiene in each experiment that are essentially identical, such that independent values of α and β cannot be determined from these data alone. An additional experiment was therefore carried out with $[O_2]/[NO_x] \approx 100$ (experiment F, Table 2). Under these conditions, the NO_2-initiated chemistry is expected to be fully terminated by reactions 27b, 25, and 28, such that generation of HO_x radicals does not occur. The observed time dependence of NO_2 and 2,4-hexadiene (see Figure 12) confirmed that removal of 2,4-hexadiene was due solely to its reaction with NO_2. Reactions 27b, 25, and 28 are each expected to yield organic products containing two oxidized nitrogen groups, such that each initiation event leads to loss of two NO_x molecules [in the case of reaction 28, the expected product is the nitrite, $CH_3CH(NO_2)CH{=}CHC(ONO)CH_3$]. However, significant regeneration of NO_x was observed, particularly in the early stages of the experiment, with the removal stoichiometry, $\Delta[NO_x]/\Delta$[2,4-hexadiene], at the end of the experiment being ca. 0.8. As shown in Figure 12, a simulation using the mechanism in Table 1 with reaction 28 leading to the expected nitrite product provided concentration−time traces for NO_2 (and therefore 2,4-hexadiene) that were in very poor agreement with observation, the main problem being too much NO_x loss. The simulation was significantly improved if reaction 28 was assumed to lead to complete release of oxidized nitrogen in the form of NO_2, i.e.

$$CH_3CH(NO_2)CH{=}CHCH(O)CH_3 + NO \rightarrow \rightarrow NO_2 + NO_2 + \text{organic product(s)} \quad (28')$$

This is because NO provides the major reaction partner for the oxy radical throughout the experiment. At longer times, $[NO_2]/[NO]$ increases and the contribution of reaction 25 to the loss of the oxy radical is therefore greater, consistent with the

observed elevated loss of NO_x in the system in the latter stages of the experiment. It is difficult to identify an alternative explanation for these observations, although the details of the mechanism of the postulated reaction (eq 28′) are not clear from the present data. It should be noted that the products assumed for reaction 28 have a substantial influence on simulations of experiment F: however, the effect under the conditions of experiments A−E, at much higher $[O_2]/[NO_x]$, is negligible.

The high degree of NO_x regeneration observed in experiment F also clearly indicates that reaction 27 needs to be largely propagating. With the assumption that reaction 28′ is a valid representation, it was possible to derive a value of $\alpha = 0.23$ from nonlinear least-squares fitting to the NO_2 and 2,4-hexadiene data (see Figure 12). In conjunction with the results of the studies in 700 Torr of O_2 presented above, we therefore assign recommended values of 0.25 ± 0.05 to both α and β.

4. Conclusions and Atmospheric Implications

A substantial body of experimental data is presented concerning the atmospheric chemistry of 2,4-hexadiene. On the basis of k(OH + 2,4-hexadiene) = $(1.76 \pm 0.58) \times 10^{-10}$ cm^3 molecule^{-1} s^{-1} reported here and a typical ambient OH radical concentration of 10^6 molecule cm^{-3}, a lifetime of 2,4-hexadiene with respect to reaction with OH radicals of ca. 1.5 h can be estimated. Reaction with ozone also occurs rapidly. Using a rate constant of 3.4×10^{-16} cm^3 molecule^{-1} s^{-1} (average of results for cis,trans and trans,trans isomers reported in ref 26) and a typical background ozone level of 40 ppb leads to a lifetime of 2,4-hexadiene with respect to reaction with ozone of ca. 1 h. Polluted urban air typically contains NO_2 concentrations of ca. 50−100 ppb, although concentrations of several hundred parts per billion have been reported during wintertime pollution episodes.[38] Using $k(NO_2 + 2,4\text{-hexadiene}) = (3.11 \pm 0.18) \times 10^{-19}$ cm^3 molecule^{-1} s^{-1}, reported here, a lifetime of 2,4-hexadiene with respect to reaction with NO_2 of ca. 15−30 days can be estimated for the typical polluted conditions. Reaction with NO_2 is therefore a negligible sink for 2,4-hexadiene under the vast majority of ambient conditions and only potentially makes a minor contribution under extreme wintertime episode conditions when a shallow inversion layer can lead to a combination of high NO_x levels and stagnant air for periods of a day or more.[38,39] Under such conditions, ozone and OH are suppressed to very low levels. Under more typical conditions, however, the atmospheric lifetime of 2,4-hexadiene is determined by the reactions with OH radicals and ozone and is likely to be less than 1 h in most environments.

The formation of acetaldehyde, *trans*-crotonaldehyde, and 2,5-dimethylfuran during the photolysis of 2,4-hexadiene/CH_3ONO/NO/O_2 mixtures suggests that the OH-initiated oxidation of 2,4-hexadiene proceeds, at least partially, by pathways analogous to those reported for 1,3-butadiene and isoprene following the initial addition of OH. However, these detected products account for only ca. 25% of the reacted carbon. Additional major contributions are expected from hydroxyhexenyl ketones and nitrates, with minor contributions from products resulting from H-atom abstraction from the terminal CH_3 groups (i.e., hexadienyl nitrates and ketones). A mechanism for the OH radical-initiated oxidation of 2,4-hexadiene has been developed and is presented in Figure 3 and Table 1.

The results of the NO_2-initiated study in the absence of O_2 are consistent with sequential addition of two NO_2 molecules to form one or more dinitrohexene isomers. In the presence of O_2, the results suggest that formation of nitrohexenyl peroxy radicals occurs. On the basis of kinetics considerations, and the observed high yield of HO_x radicals in the presence of NO, it is postulated that the chemistry proceeds predominantly via formation of the 2-nitro-3-hexenyl-5-peroxy isomer, which undergoes conventional peroxy radical reactions (i.e. with NO, NO_2, and peroxy radicals).

When NO is present, the NO_2-initiated oxidation leads to NO-to-NO_2 conversion and the formation of HO_x radicals in significant yield. The present results are consistent with an HO_x yield of 0.75 ± 0.05 at typical urban levels of NO_x. These results are also consistent with the reported generation of OH from the NO_2-initiated oxidation of 1,3-cyclohexadiene.[7] The present work thus also supports the general features of the mechanism postulated by Shi and Harrison[3] for 1,3-cyclohexadiene and 1-methyl-1,3-cyclopentadiene and the potential of conjugated diene/NO_2 reactions to promote NO to NO_2 oxidation in samples of diluted vehicle exhaust and fuel vapor. However, it is not possible to assess the relative importance of these reactions for the generation of HO_x radicals in the polluted urban environment without further quantitative measurements of the ambient concentrations of conjugated dienes.

Acknowledgment. M.E.J. acknowledges the U.K. Natural Environment Research Council, NERC, for support via a Senior Research Fellowship (NER/K/S/2000/00870). We thank Ole John Nielsen (Copenhagen University) for helpful discussions.

Appendix: Allowance for N_2O_4 Formation in the Calibrated Volume

Consider the equilibrium

$$N_2O_4 \rightleftarrows NO_2 + NO_2$$

$$K_P = \frac{[NO_2]^2}{[N_2O_4]} = \frac{(P_{NO_2}/P_0)^2}{(P_{N_2O_4}/P_0)}$$

where P_0 = standard pressure (1 atm). Let α be the degree of dissociation and P be the total pressure of the $NO_2 + N_2O_4$ sample:req:

$$P_{NO_2} = \left(\frac{2\alpha}{1+\alpha}\right)P \qquad P_{N_2O_4} = \left(\frac{1-\alpha}{1+\alpha}\right)P \qquad K_P = \frac{4\alpha^2 P/P_0}{1-\alpha^2}$$

$$\therefore \alpha^2 = \frac{K_P}{K_P + 4P/P_0}$$

where $\Delta G = -RT \ln K_P = 5.33$ kJ mol^{-1} at 295 K.[40]

Hence, the degree of dissociation of N_2O_4 in the gas mixture can be calculated from

$$\alpha^2 = \frac{0.114}{0.114 + 4P/P_0}$$

The sample $N_2O_4 + NO_2$ pressure, P, in the calibrated volume was 2.0−12.7 Torr. Under these conditions a significant fraction of the NO_2 is present in the form of the dimer, N_2O_4. For example, with $P = P_{N_2O_4} + P_{NO_2} = 12.7$ Torr, the degree of dissociation of N_2O_4 (α) is 0.79. On expansion into the chamber, the dimer dissociates, and hence the pressure of NO_2 in the chamber is a factor of 1.21 ($2 - \alpha$) higher than that calculated from Boyle's law from the pressure, P, in the calibrated volume.

References and Notes

(1) Guenther, A.; Hewitt, C. N.; Erickson, D.; Fall, R.; Geron, C.; Graedel, T.; Harley, P.; Klinger, L.; Lerdau, M.; McKay, W. A.; Pierce,

T.; Scholes, B.; Steinbrecher, R.; Tallamraju, R.; Taylor, J.; Zimmerman, P. *J. Geophys. Res.* **1995**, *100*, 8873−8892.

(2) Jemma, C. A.; Shore, P. R.; Widdicombe, K. A. *J. Chromatogr. Sci.* **1995**, *33*, 34−48.

(3) Shi, J. P.; Harrison, R.„M. *Atmos. Environ.* **1997**, *31*, 3857−3866.

(4) Smith, D.; Cheng, P.; Spaněl, P. *Rapid Commun. Mass Spectrosc.* **2002**, *16*, 1124−1134.

(5) Ciccioli, P.; Cecinato, A.; Brancaleoni, E.; Brachetti, A.; Frattoni, M.; Sparapani, R. Composition and distribution of polar and nonpolar VOCs in urban, rural, forest and remote areas. In Proceedings of the 6th European symposium on the physicochemical behaviour of atmospheric pollutants, Varese, 18−22 October 1993; pp 549−568; Report EUR 15609/1 EN, 1994 (ISBN 92-826-7922-5).

(6) Calvert, J. G.; Atkinson, R.; Kerr, J. A.; Madronich, S.; Moortgat, G. K.; Wallington, T. J.; Yarwood, G. *The mechanisms of atmospheric oxidation of alkenes*; Oxford University Press: New York, 2000 (ISBN 0-19-513177-0).

(7) Atkinson, R.; Aschmann, S. M.; Winer, A. M.; Pitts, J. N., Jr. *Int. J. Chem. Kinet.* **1984**, *16*, 697−706.

(8) Tuazon, E. C.; Atkinson, R. *Int. J. Chem. Kinet.* **1990**, *22*, 1221−1236.

(9) Harrison, R. M.; Shi, J. P.; Grenfell, J. L. *Atmos. Environ.* **1998**, *32*, 2769−2774.

(10) King, M. D.; Canosa-Mas, C. E.; Wayne, R. P. *Phys. Chem. Chem. Phys.* **2000**, *4*, 295−303.

(11) Tuazon, E. C.; Alvarado, A.; Aschmann, S. M.; Atkinson, R.; Arey, J. *Environ. Sci. Technol.* **1999**, *33*, 3586−3595.

(12) Liu, X.; Jeffries, H. E.; Sexton, K. G. *Atmos. Environ.* **1999**, *33*, 3005−3022.

(13) Atkinson, R.; Aschmann, S. M.; Tuazon, E. C.; Arey, J.; Zelinska, B. *Int. J. Chem. Kinet.* **1989**, *21*, 593−604.

(14) Paulson, S. E.; Flagan, R. C.; Seinfeld, J. H. *Int. J. Chem. Kinet.* **1992**, *24*, 79−101.

(15) Miyoshi, A.; Hatakeyama, S.; Washida, N. *J. Geophys. Res.* **1994**, *99*, 18779−18787.

(16) Kwok, E. S. C.; Atkinson, R.; Arey, J. *Environ. Sci. Technol.* **1995**, *29*, 2467−2469.

(17) Ruppert, L.; Becker, K. H. *Atmos. Environ.* **2000**, *34*, 1529−1542.

(18) Wallington, T. J.; Japar, S. M. *J. Atmos. Chem.* **1989**, *9*, 399−409.

(19) Calvert, J. G.; Atkinson, R.; Becker, K. H.; Kamens, R. M.; Seinfeld, J. H.; Wallington, T. J.; Yarwood, G. *The mechanisms of atmospheric oxidation of aromatic hydrocarbons*; Oxford University Press: New York, 2002 (ISBN 0-19-514628-X).

(20) Ohta, T. *J. Phys. Chem.* **1983**, *87*, 1209−1213.

(21) Atkinson, R. *J. Phys. Chem. Ref. Data* **1997**, *26*(2), 215.

(22) Jenkin, M. E.; Boyd, A. A.; Lesclaux, R. *J. Atmos. Chem.* **1998**, *29*, 267−298.

(23) Peeters, J.; Vandenberk, S.; Piessens, E.; Pultau V. *Chemosphere* **1999**, *38*(6), 1189−1195.

(24) Vereecken, L.; Peeters, J. *Chem. Phys. Lett.* **2001**, *333*, 162−168.

(25) Lightfoot, P. D.; Cox, R. A.; Crowley, J. N.; Destriau, M.; Hayman, G. D.; Jenkin, M. E.; Moortgat, G. K.; Zabel, F. *Atmos. Environ.* **1992**, *26A*, 1805−1964.

(26) Atkinson, R. *Int. J. Chem. Kinet.* **1997**, *29*, 99−111.

(27) Grotheer, H. H.; Riekert, G.; Walter, D.; Just, T. *J. Phys. Chem.* **1988**, *92*, 4028−4030.

(28) Nesbitt, F. L.; Payne, W. A.; Stief, L. J. *J. Phys. Chem.* **1988**, *92*, 4030−4032.

(29) Pagsberg, P.; Munk, J.; Anastasi, C.; Simpson, V. J. *J. Phys. Chem.* **1989**, *93*, 5162−5165.

(30) Miyoshi, A.; Matsui, H.; Washida, N. *J. Phys. Chem.* **1990**, *94*, 3016−3019.

(31) Moortgat, G. K.; Cox, R. A.; Schuster, G.; Burrows, J. P.; Tyndall, G. S. *J. Chem. Soc., Faraday Trans.* **1989**, *85*(7), 809−829.

(32) Veyret, B.; Lesclaux, R.; Rayez, M. T.; Rayez, J. C.; Cox, R. A.; Moortgat, G. K. *J. Phys. Chem.* **1989**, *93*, 2368−2374.

(33) Saunders, S. M.; Jenkin, M. E.; Derwent, R. G.; Pilling, M. J. *Atmos. Chem. Phys. Discuss.* **2002**, *2*, 1847−1903.

(34) Ohta, T.; Nagura, H.; Suzuki, S. *Int. J. Chem. Kinet.* **1986**, *18*, 1−11.

(35) Glasson, W. A.; Tuesday, C. S. *Environ. Sci. Technol.* **1970**, *4*, 752−757.

(36) Lesclaux, R. Combination of peroxyl radicals in the gas phase. In *Peroxyl Radicals*; Alfassi, Z. B., Ed.; John Wiley and Sons: Chichester, U.K., 1997.

(37) Atkinson, R.; Baulch, D. L.; Cox, R. A.; Hampson, R. F.; Kerr, J. A.; Rossi, M. J.; Troe, J. *Summary of evaluated kinetic and photochemical data for atmospheric chemistry*; IUPAC sub-committee on gas kinetic data evaluation for atmospheric chemistry; accessed from http://www.iupac-kinetic.ch.cam.ac.uk, 2000.

(38) Bower, J. S.; Broughton, G. F. J.; Stedman, J. R.; Williams, M. L. *Atmos. Environ.* **1994**, *28*(3), 461−475.

(39) QUARG. *Urban air quality in the United Kingdom*; First report of the Quality of Urban Air Review Group, prepared at the request of the Department of the Environment, London, 1993.

(40) Harris and Churney. *J. Chem. Phys.* **1967**, *47*, 1703−1709.